JOURNAL OF VIROLOGY, Nov. 2009, p. 11402–11406 Vol. 83, No. 21
0022-538X/09/$12.00 doi:10.1128/JVI.00504-09

Characterization of a Mumps Virus Nucleocapsidlike Particle[▽]

Robert Cox,[1] Todd J. Green,[1] Shihong Qiu,[1] Jungsoon Kang,[1] Jun Tsao,[1] Peter E. Prevelige,[1] Biao He,[2] and Ming Luo[1]*

Department of Microbiology, University of Alabama at Birmingham, 1025 18th Street South, Birmingham, Alabama 35294,[1] and Department of Veterinary and Biomedical Sciences, Pennsylvania State University, University Park, Pennsylvania 16802[2]

Received 11 March 2009/Accepted 7 August 2009

The nucleocapsid protein (NP) of mumps virus (MuV), a paramyxovirus, was coexpressed with the phosphoprotein (P) in *Escherichia coli*. The NP and P proteins form a soluble complex containing RNA. Under a transmission electron microscope, the NP-RNA complex appears as a nucleocapsidlike ring that has a diameter of approximately 20 nm with 13 subunits. There is a piece of single-stranded RNA with a length of 78 nucleotides in the NP-RNA ring. Shorter RNA pieces are also visible. The MuV NP protein may provide weaker protection of the RNA than the NP protein of some other negative-strand RNA viruses, reflecting the degree of NP protein association.

Mumps virus (MuV) is the cause of an acute, but usually non-life-threatening, infection which occurs most frequently in childhood or adolescence. MuV belongs to the family *Paramyxoviridae*, genus *Rubulavirus*. The MuV genome consists of one nonsegmented single-stranded RNA molecule with seven negative-sense genes encoding eight proteins in the following order: the nucleocapsid protein (NP), V protein (V)/phosphoprotein (P), matrix protein (M), fusion protein (F), small hydrophobic protein (SH), hemagglutinin-neuraminidase (HN), and large (L) protein.

The MuV NP protein is 549 amino acids in length and is composed of an N-terminal domain and a reportedly unstructured C-terminal tail (11). The N-terminal domain is suggested to be the part mainly responsible for RNA encapsidation, P protein binding, and formation of the nucleocapsid (10, 11). The primary function of the NP protein of a negative-strand RNA virus (NSRV) is to form the viral nucleocapsid by encapsidating the viral genomic RNA during replication. Crystal structures of nucleocapsidlike NP-RNA complexes have been solved for vesicular stomatitis virus (VSV) and rabies virus (RABV) (1, 7). The crystal structure shows that the NP proteins line up side by side to form a continuous capsidlike structure, with the RNA accommodated in a central tunnel in the capsid. The nonsegmented NSRVs encode their own viral polymerases, a complex composed of the L and P proteins. In order to allow the polymerase to access the RNA template during viral transcription or replication, the nucleocapsid must undergo some conformational change to expose the RNA. It is expected that MuV NP has some similarity with these previously determined structures; however, differences are expected since the nucleocapsid template of a paramyxovirus follows a strict "rule of six," i.e., the length of the viral genome needs to be an integer of six nucleotides in order to serve as a fully functional template (12).

A single vector was constructed to coexpress the MuV NP and P proteins in *Escherichia coli* at equal molar ratios by following the approach of Green et al. (6). Soluble N-terminally His-tagged P protein could be copurified with the NP protein by affinity chromatography. When the loaded Ni affinity column was briefly washed with a buffer (20 mM Tris [pH 7.9], 500 mM NaCl, 50 mM imidazole), a portion of the NP protein was found to elute from the column (Fig. 1A, lane 4). However, a significant fraction of the NP protein remained bound in the column. The NP-P complex was found to elute from the Ni affinity column at a concentration of approximately 150 mM imidazole.

The fraction eluted by a mild wash was purified by ion-exchange chromatography (HiTrap Q HP; GE Healthcare) (Fig. 1B). Fractions containing the NP protein were further purified by size exclusion chromatography using a Sephacryl S-300 column (GE Healthcare) (Fig. 1E). The NP protein was mostly in fractions corresponding to molecular masses larger than 300,000 Da, suggesting the presence of a complex much larger than the monomeric protein. Recombinant nucleocapsidlike ring structures were previously observed for VSV, RABV, and respiratory syncytial virus (RSV) (1, 2, 6). It is therefore logical to suspect that this fraction of the MuV NP protein is also a nucleocapsidlike ring.

The purified MuV NP protein fraction was examined under EM using an FEI Technai Spirit electron microscope (EM) at the high-resolution imaging facility at the University of Alabama at Birmingham (Fig. 2). The EM images clearly showed that the majority of the MuV NP protein is in the form of a ring similar to those observed for VSV, RABV, and RSV NP-RNA complexes (6, 9, 15). A collection of isolated ring images were averaged using the program EMAN (14). Since almost all the images were taken down the central axis of the ring structures and no tilt of the grids was applied during imaging, the averaging was carried out with only two-dimensional images. To build an initial model, 1,173 images were collected and averaged. Among different rotation axes, the 13-fold axis (C13) produced the best averaged image. Using this model, a final collection of 445 images was used to generate a three-dimensional model for the MuV NP-RNA ring (Fig. 2B). The outer diameter measured for the averaged ring structure is 20.0 nm,

* Corresponding author. Mailing address: Room 111, CBSE, 1025 18th Street South, University of Alabama at Birmingham, Birmingham, AL 35294. Phone: (205) 934-4259. Fax: (205) 975-9578. E-mail: mingluo@uab.edu.

▽ Published ahead of print on 19 August 2009.

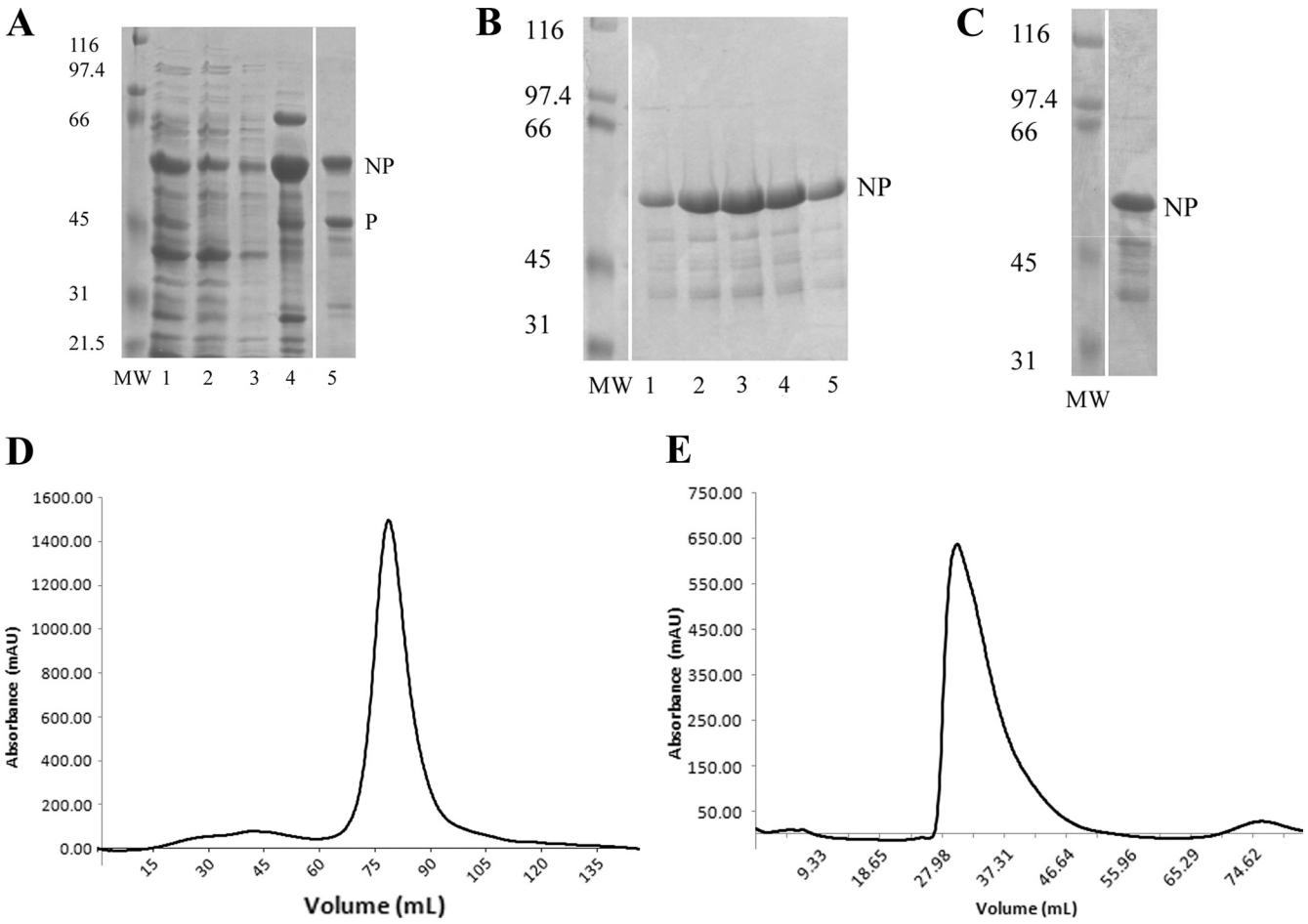

FIG. 1. MuV NP and P proteins were coexpressed in *E. coli* and purified as described in the text. (A) Lanes 1 to 4 represent total soluble proteins postinduction, in the Ni column flowthrough, in the binding buffer wash, and in the washing buffer wash of the Ni column, respectively. Lane 5 shows a fraction containing the NP-P complex eluted by the linear imidazole gradient from the Ni affinity column. (B) The washing buffer wash contained a large amount of NP protein. It was dialyzed to 200 mM NaCl and further purified on a HiTrap Q HP (GE Healthcare) ion-exchange column. Lanes 1 to 5 contain the MuV NP-RNA complex. (C) Fractions containing the NP-RNA complex from the ion-exchange column were further purified by size exclusion chromatography. Lanes 1 and 2 represent the molecular weight markers (in thousands) and fractions containing the MuV NP-RNA complex, respectively. (D) Profile of MuV NP-RNA eluting from the ion-exchange column. The largest peak represents the NP-RNA complex. (E) Profile of MuV NP-RNA eluting from the size exclusion column. The single large peak represents the NP protein.

and the inner diameter is 5.6 nm. The thickness of the ring is 6.7 nm. The shape of the ring, with one end narrower than the other, is similar to the shape of rings of other nucleocapsidlike particles. This number of subunits, 13, is consistent with that of the twist in the nucleocapsid of measles virus, another member of paramyxovirus family; the diameter of the ring and its hollow center are consistent with those of the nucleocapsid of measles virus (3).

To confirm the size determined with the averaged EM image, the sedimentation coefficient ($s_{20,w}$) was determined to be 32.191 S by ultracentrifugation by using the programs Sednterp and Sedfit (13, 18) (Fig. 2C). The molecular mass calculated from the sedimentation coefficient is 853,000 Da. This molecular mass is within the experimental error when it is compared to the calculated molecular mass of a 13-subunit MuV NP-RNA ring (830,960 Da), assuming that the molecular mass of a MuV NP subunit is 62 kDa and that of six nucleotides per subunit is 1.92 kDa.

Similar structures of other recombinant NSRV NP protein complexes often contain encapsidated RNA. We measured the ratio of the optical density at 260 nm to that at 280 nm for the MuV NP protein complex and found the value to be 1.26, indicating that the MuV NP protein complex has encapsidated RNA. To characterize the encapsidated RNA, materials extracted with Trizol (Invitrogen) from the purified NP protein complex were examined by electrophoresis under denaturing conditions (Fig. 3A, lane 4). The gel clearly showed that RNA is present in the complex. However, the length of RNA is more variable than what has been observed for the VSV, RABV, or RSV NP-RNA complexes (6, 9, 19). Assuming that each NP subunit accommodates six nucleotides, the RNA in a fully occupied 13-subunit ring of the MuV NP-RNA complex should have a length of 78 nucleotides. In fact, a dominant RNA band corresponding to this length was shown in the RNA gel (Fig. 3A, lane 4, band I). Additionally, a large number of RNA pieces smaller than band I were observed (Fig. 3A). The ap-

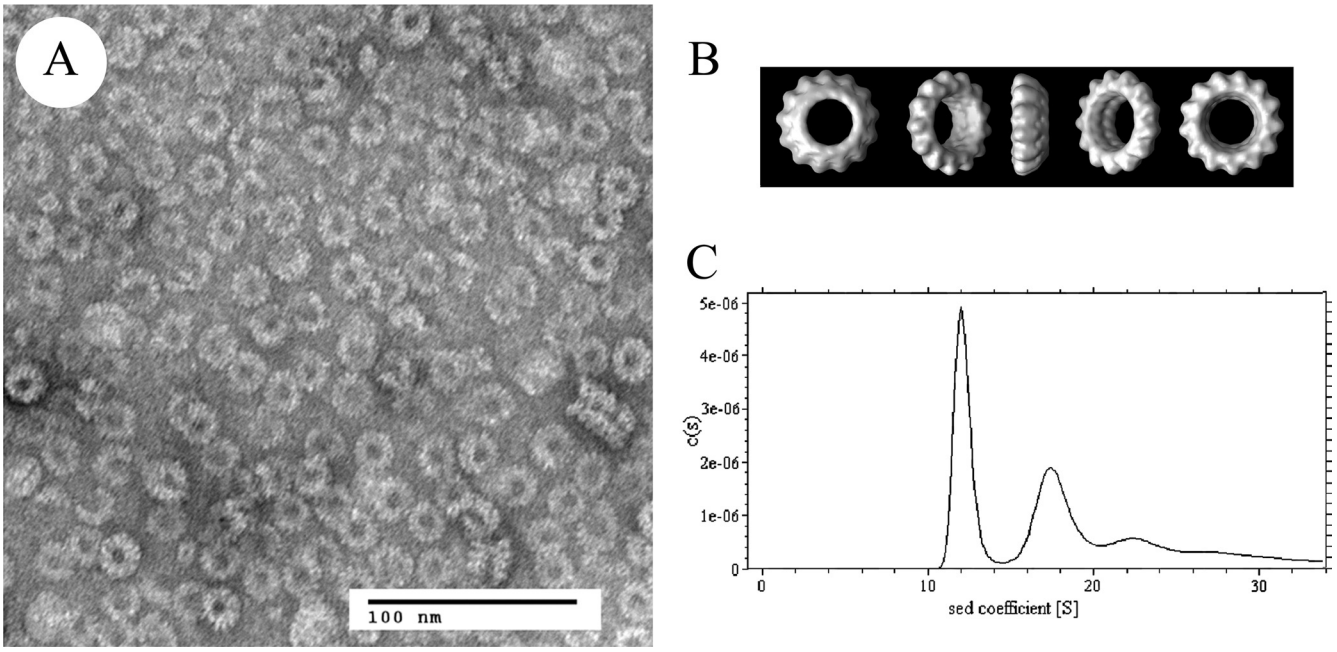

FIG. 2. The number of MuV NP protein subunits per nucleocapsid ring was determined by EM analysis and analytical ultracentrifugation experiments. (A) A typical EM image of negatively stained MuV NP-RNA (50 mM Tris [pH 7.5], 470 mM NaCl). (B) Particles were selected, and a three-dimensional model was generated from 445 views of MuV nucleocapsidlike rings. The average internal and external diameters are 5.6 nm and 20.0 nm, respectively, and the thickness of the ring is 6.7 nm. The number of subunits per nucleocapsidlike ring was determined to be 13. The resolution was determined at a Fourier shell correlation of 0.5 to be 24 Å. The statistics of image reconstruction are as follows: mean = −0.084843; standard deviation = 0.98878; root mean square = 0.99241; contour level = 2.71; subsampling interval = 2 Å. The image was displayed with Chimera (16). (C) The number of molecules per nucleocapsidlike ring was verified by analytical ultracentrifugation. Band profiles suggested a dominant single species, and the sedimentation is consistent with a ring with 13 NP subunits. Sed., sedimentation.

pearance of a dominant band, band II, which was actually part of a population of small RNA pieces, could be an artifact of ethidium bromide or SYBR gold (Invitrogen) staining. This observation suggests that the RNA piece encapsidated by the MuV NP protein during heterologous expression was not fully protected during purification, which is supported by the observation that the RNA in the MuV N-RNA complex is susceptible to digestion when incubated with RNase A for 1 h at 37°C (Fig. 3A, lane 6).

In order to determine the effect of pH, salt, and temperature on the susceptibility of NP-bound RNA, the MuV NP-RNA ring was incubated under a variety of different conditions. The

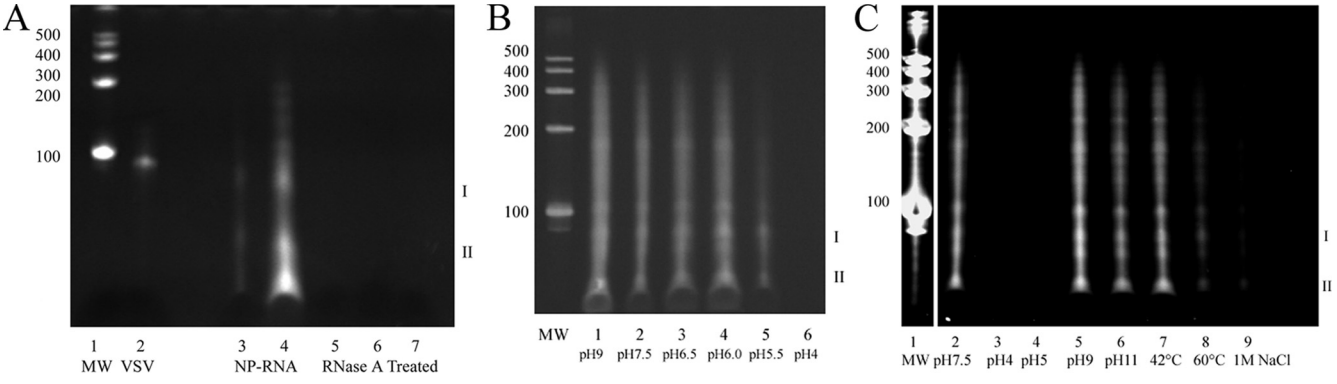

FIG. 3. The MuV nucleocapsidlike particles contain RNA. The length of the RNA encapsidated in the MuV NP ring was measured by comparison with the RNA molecular weight marker (Century Marker; Ambion). (A) RNA was extracted from purified VSV NP-RNA complex (lane 2), the MuV NP-RNA complex (lanes 3 and 4), and RNase A-treated MuV NP protein incubated at pH 7.5 (lane 6). The gel was stained with ethidium bromide. Two RNA bands are labeled I and II. (B and C) Purified samples of the MuV NP-RNA complex were incubated for 1 h under different buffer conditions. The samples were then returned to normal buffer conditions (50 mM Tris [pH 7.5], 470 mM NaCl) and allowed to incubate overnight at 8°C. RNA was extracted using Trizol (Invitrogen), and samples were analyzed in a 10% 8 M urea-polyacrylamide gel. Both gels were stained with SYBR gold (Invitrogen). (B) Lanes 1 to 6 correspond to the MuV NP-RNA complex incubated at pH 9, pH 7.5, pH 6.5, pH 6.0, pH 5.5, and pH 4.0, respectively. (C) Lanes 1 to 9 correspond to MW Marker (Century Marker; Ambion) and MuV NP-RNA complex incubated at pH 7.5, pH 4, pH 5, pH 9, pH 11, 42°C, 60°C, and MuV NP-RNA complex in 1 M NaCl (pH 8.3), respectively.

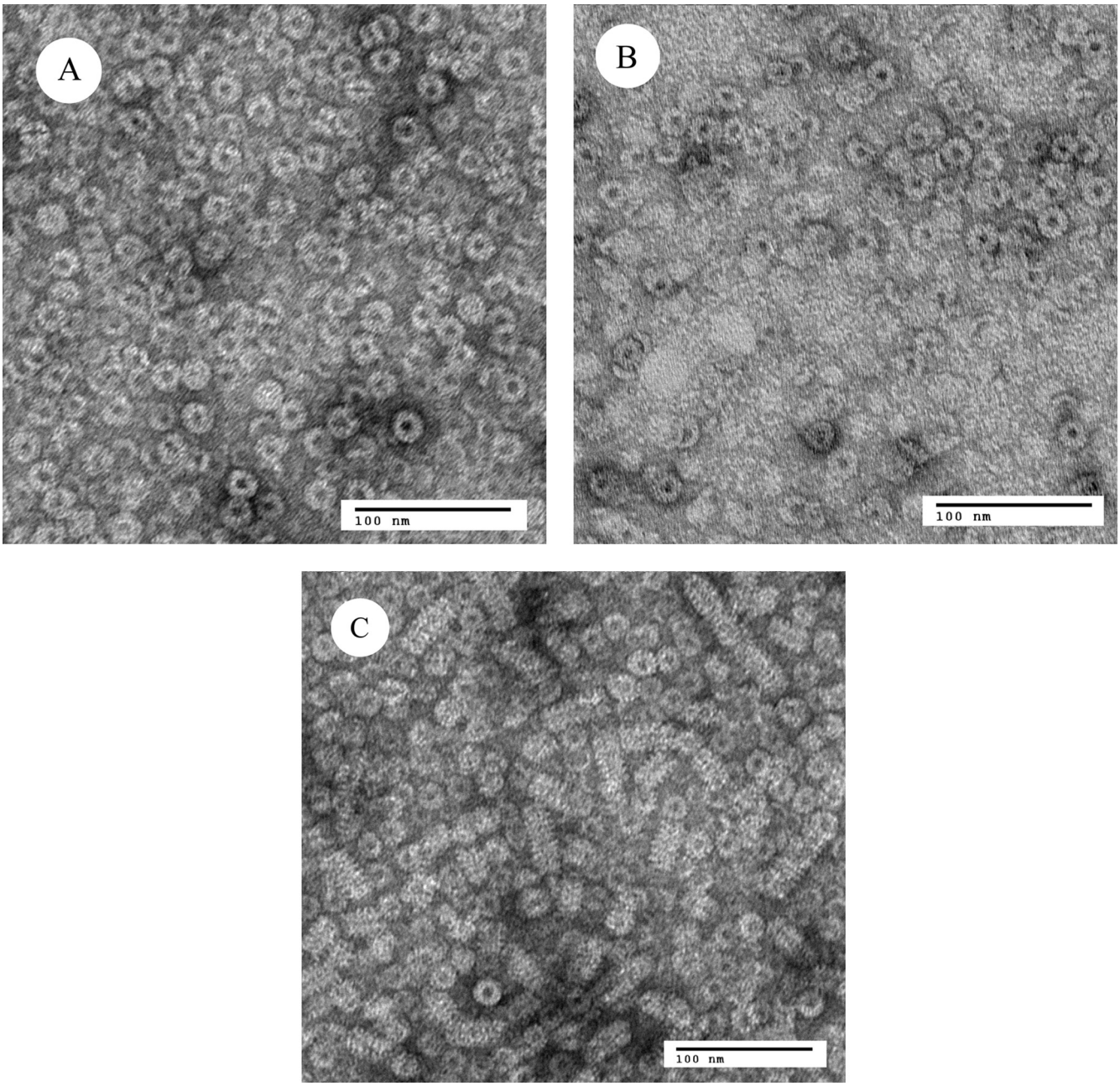

FIG. 4. EMs of the MuV NP-RNA complex were negatively stained with 2% uranyl acetate (magnification, ×42,000). (A) The MuV NP-RNA complex incubated in 50 mM Tris pH 8.3 plus 1 M NaCl; (B) the MuV NP-RNA complex as a precipitant in 0.1 M citric acid-sodium citrate (pH 4) plus 470 mM NaCl; (C) the MuV NP-RNA complex incubated at pH 4 and resolubilized by increasing the pH back to approximately 7.5. The ring structures in panels A, B, and C were comparable to that of the untreated MuV NP-RNA ring (Fig. 2A) after the RNA was lost. These ring structures could be considered "empty-capsid"-like structures. The scale bar in the bottom right corner of each micrograph corresponds to 100 nm.

conditions examined included pH 4, pH 4.5, pH 5, pH 5.5, pH 6.0, pH 6.5, pH 7.5, pH 9, pH 11, 1 M NaCl, 2 M NaCl, 42°C, and 60°C. The NP-RNA ring was incubated for 1 h under each condition and then returned to normal buffer conditions (50 mM Tris [pH 7.5], 470 mM NaCl). The NP-RNA ring was then allowed to incubate overnight at 8°C, and RNA was extracted using Trizol (Fig. 3B and C). It was found that the RNA contained in the MuV NP-RNA complex is highly susceptible to digestion by contaminant nucleases under several of these conditions. After incubation at a pH lower than 5, all RNA pieces were lost. This level of RNA protection is significantly less than that of the VSV NP-RNA ring (6). At a pH above 6, no further loss of RNA was observed, which is similar to findings with the VSV and RABV NP-RNA rings (6, 9). When the MuV NP-RNA ring was subjected to 1 M NaCl, the RNA was also lost, similar to the situation when the nucleocapsid of influenza A virus was treated with high salt concentrations (8). The RNA in the VSV or RABV NP-RNA complex was not

affected by high salt concentrations (6, 9). Finally, the RNA was lost when the MuV NP-RNA ring was heated to 60°C for 1 hour. No information on heat treatment of other NSRV NP-RNA rings was available at the time this study was done. The loss of RNA at a pH of less than 5.0 or under high-salt or high-temperature conditions suggested that associations between the MuV NP subunits may be weaker than between the NP subunits of other NSRVs.

EM images were taken of samples that had been subjected to different conditions as described above (Fig. 4). These images (Fig. 4A and B) showed that the loss of RNA from the MuV NP-RNA ring after various treatments was not due to denaturation of the NP protein. The ring structures remained intact after RNA was lost and looked like untreated MuV NP-RNA rings. These ring structures could be considered "empty-capsid"-like structures. One interesting observation is that the MuV empty-capsid-like rings formed rodlike structures after being subjected to pH 4.0 and then reneutralized (Fig. 4C). It seems that the MuV rings could easily make top-and-bottom interactions as would be present in the superhelical structure of the paramyxovirus nucleocapsid (4, 17).

Several NSRV nucleocapsidlike rings have recently been described (2, 7, 9). Coexpression of the MuV NP and P proteins in *E. coli* has resulted in the production of nucleocapsid-like rings with morphologies similar to those seen in other NSRVs. The MuV NP-RNA ring contains 13 NP subunits and contains RNA. There are multiple sizes of RNA contained within the NP ring, which is not seen with other NSRVs such as the NP-RNA ring of VSV, suggesting that the RNA in the MuV NP ring is less protected (6). The study of the MuV nucleocapsidlike particle will lead to further understanding of the unique features of the paramyxovirus nucleocapsid.

This work is supported in part by National Institutes of Health grant AI050066 to M.L. and grant AI-065795 to B.H.

REFERENCES

1. **Albertini, A. A., A. K. Wernimont, T. Muziol, R. B. Ravelli, C. R. Clapier, G. Schoehn, W. Weissenhorn, and R. W. Ruigrok.** 2006. Crystal structure of the rabies virus nucleoprotein-RNA complex. Science **313:**360–363.
2. **Bhella, D., A. Ralph, L. B. Murphy, and R. P. Yeo.** 2002. Significant differences in nucleocapsid morphology within the Paramyxoviridae. J. Gen. Virol. **83:**1831–1839.
3. **Bhella, D., A. Ralph, and R. P. Yeo.** 2004. Conformational flexibility in recombinant measles virus nucleocapsids visualised by cryo-negative stain electron microscopy and real-space helical reconstruction. J. Mol. Biol. **340:** 319–331.
4. **Bourhis, J. M., B. Canard, and S. Longhi.** 2006. Structural disorder within the replicative complex of measles virus: functional implications. Virology **344:**94–110.
5. Reference deleted.
6. **Green, T. J., S. Macpherson, S. Qiu, J. Lebowitz, G. W. Wertz, and M. Luo.** 2000. Study of the assembly of vesicular stomatitis virus N protein: role of the P protein. J. Virol. **74:**9515–9524.
7. **Green, T. J., X. Zhang, G. W. Wertz, and M. Luo.** 2006. Structure of the vesicular stomatitis virus nucleoprotein-RNA complex. Science **313:**357–360.
8. **Heggeness, M. H., P. R. Smith, I. Ulmanen, R. M. Krug, and P. W. Choppin.** 1982. Studies on the helical nucleocapsid of influenza virus. Virology **118:** 466–470.
9. **Iseni, F., A. Barge, F. Baudin, D. Blondel, and R. W. Ruigrok.** 1998. Characterization of rabies virus nucleocapsids and recombinant nucleocapsid-like structures. J. Gen. Virol. **79:**2909–2919.
10. **Kingston, R. L., W. A. Baase, and L. S. Gay.** 2004. Characterization of nucleocapsid binding by the measles virus and mumps virus phosphoproteins. J. Virol. **78:**8630–8640.
11. **Kingston, R. L., L. S. Gay, W. S. Baase, and B. W. Matthews.** 2008. Structure of the nucleocapsid-binding domain from the mumps virus polymerase; an example of protein folding induced by crystallization. J. Mol. Biol. **379:**719–731.
12. **Kolakofsky, D., L. Roux, D. Garcin, and R. W. Ruigrok.** 2005. Paramyxovirus mRNA editing, the "rule of six" and error catastrophe: a hypothesis. J. Gen. Virol. **86:**1869–1877.
13. **Laue, T. M., B. D. Shah, T. M. Ridgeway, and S. L. Pelletier.** 1992. Computer-aided interpretation of analytical sedimentation data for proteins, p. 90–125. *In* S. E. Harding, A. J. Rowe, and J. C. Horton (ed.), Analytical ultracentrifugation in biochemistry and polymer science. Royal Society of Chemistry, Cambridge, United Kingdom.
14. **Ludtke, S. J., P. R. Baldwin, and W. Chiu.** 1999. EMAN: semiautomated software for high-resolution single-particle reconstructions. J. Struct. Biol. **128:**82–97.
15. **Maclellan, K., C. Loney, R. P. Yeo, and D. Bhella.** 2007. The 24-angstrom structure of respiratory syncytial virus nucleocapsid protein-RNA decameric rings. J. Virol. **81:**9519–9524.
16. **Pettersen, E. F., T. D. Goddard, C. C. Huang, G. S. Couch, D. M. Greenblatt, E. C. Meng, and T. E. Ferrin.** 2004. UCSF Chimera: a visualization system for exploratory research and analysis. J. Comput. Chem. **25:**1605–1612.
17. **Schoehn, G., M. Mavrakis, A. Albertini, R. Wade, A. Hoenger, and R. W. Ruigrok.** 2004. The 12 Å structure of trypsin-treated measles virus N-RNA. J. Mol. Biol. **339:**301–312.
18. **Schuck, P.** 2000. Size-distribution analysis of macromolecules by sedimentation velocity ultracentrifugation and Lamm equation modeling. Biophys. J. **78:**1606–1619.
19. **Tran, T. L., N. Castagne, D. Bhella, P. F. Varela, J. Bernard, S. Chilmonczyk, S. Berkenkamp, V. Benhamo, K. Grznarova, J. Grosclaude, C. Nespoulos, F. A. Rey, and J. F. Eleouet.** 2007. The nine C-terminal amino acids of the respiratory syncytial virus protein P are necessary and sufficient for binding to ribonucleoprotein complexes in which six ribonucleotides are contacted per N protein protomer. J. Gen. Virol. **88:**196–206.